

Reflective High Energy Electron Diffraction (RHEED) –



A Unique Tool for In-situ Growth Monitoring



By Oleg Maksimov,
Materials Research Institute,
Pennsylvania State University,
University Park, PA

It is well known that physical properties of oxide and semiconductor films depend on the crystalline perfection. Single crystalline, textured, and polycrystalline films of the same composition have different resistivity, index of refraction, and even band gap energy. Achieving the film with the desired properties requires a number of calibration runs followed by the extensive *ex-situ* characterization. First, crystalline structure of the films deposited by evaporation, sputtering, chemical vapor and pulsed laser deposition (CVD and PLD) is assessed using X-ray diffraction, scanning and transmission electron microscopy (SEM and TEM). Next, deposition parameters are adjusted according to the characterization results. However, this approach is extremely time consuming and often suffers from the low run-to-run reproducibility. Clearly, a technique that can be used to characterize films *in-situ* during the deposition will simplify this process significantly.

Such a technique – Reflective High Energy Electron Diffraction (RHEED) – was introduced 80 years ago [1]. However, it became widely used only in the early 80's with the development of one of the most advanced thin film growth techniques – Molecular Beam Epitaxy (MBE) [2]. The schematic of a RHEED system installed in the MBE chamber is shown in **Figure 1a**. It consists of a high-energy electron gun (10 – 30keV) directed towards the substrate surface under a small incident angle (1 - 3°). The well-collimated electron beam is diffracted by the crystalline surface and is detected by the fluorescence on the phosphorus screen. The glancing incident angle ensures that electrons penetrate only through the top few monolayers making this technique extremely surface sensitive. In addition, glancing angle keeps both electron gun and detector (phosphorous screen) well clear of the material sources, such as effusion cells in MBE and targets in PLD. Thus, crystallographic structure of the film can be studied during the deposition process.

RHEED pattern depends on the surface morphology, reconstruction, and crystal orientation. In general, four types of pattern are collected from the crystalline surface.

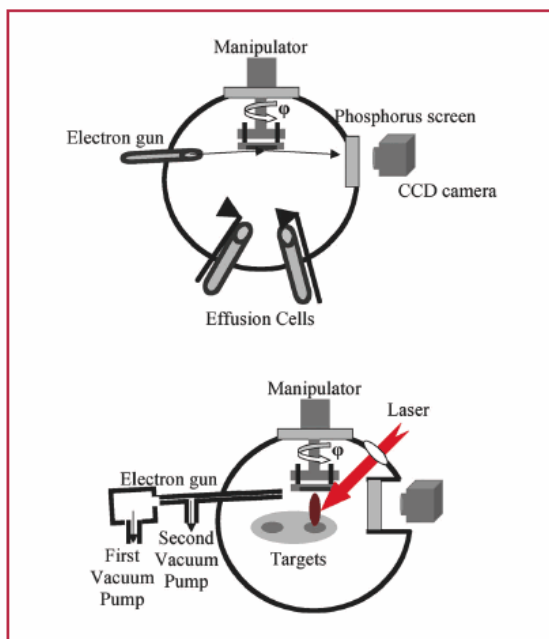


Figure 1. a) Schematic representation of a RHEED system installed in the MBE chamber. b) Schematic representation of a high-pressure RHEED system installed in the PLD chamber.

Single crystalline films with the atomically flat surface consisting of the micrometer-size terraces produce a set of sharp diffraction spots lying along the Laue rings. Only the bottom half of the zero-order ring is usually visible due to the limited size of the screen and the shadow effect from the substrate, as shown in **Figure 2a**. The geometry of the RHEED pattern can be simulated using the kinematical theory. Then, the separation between the diffraction spots (r) can be related with the reciprocal lattice (a^*) or in-plane lattice ($a_{||}$) spacing of the film through the equations:

$$r = a^* \lambda L / 2\pi$$

$$r = \lambda L / a_{||}$$

where λ is the electron energy and L is the distance between the substrate and the detector. Thus, it is possible to measure the in-plane lattice constant and, by monitoring RHEED pattern evolution, study strain relaxation during the film growth and determine its critical thickness [3,4]. Since the substrate can be rotated around the z-axis, information can be collected along different crystal directions.

Due to the crystal symmetry interruption, topmost atomic layer of the film rearranges to minimize free surface energy. This surface rearrangement, known as reconstruction, is also often visible in the RHEED as a weak superstructure. For example, a three-fold reconstruction - 3 weak lines between major diffraction spots - that is due to the ordered oxygen vacancies on the (100) TiO_2 surface is shown in **Figure 3a**. Since surface reconstructions are temperature-sensitive they, in addition to the thermocouple and pyrometer readings, are used to monitor real surface temperature and optimize growth conditions.

When the terraces decrease in size, the diffraction spots trans-

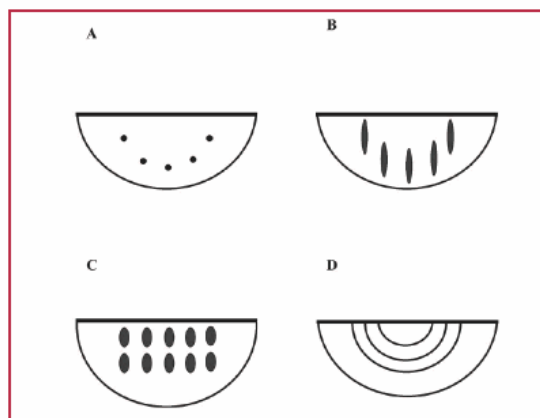


Figure 2. RHEED diffraction patterns for a) single crystalline film with the atomically flat surface consisting of the micrometer-size terraces, b) single crystalline film with the atomically flat surface consisting of the wide density of small terraces, c) single crystalline film with rough three-dimensional surface, d) polycrystalline or textured film.

form into the diffraction streaks with the streak width being inversely proportional to the terrace size, as shown in **Figure 2b**.

Single crystalline films with rough three-dimensional surface produce transmission pattern – the electron beam now penetrates through the crystallites - a set of broad spots, as shown in **Figure 2c**. This pattern is usually observed during the growth of the strongly lattice mismatched materials – when the film grows via island (Volmer-Weber) or layer plus island (Stranski-Krastanov) mode. A transition from the diffraction streaks to the transmission spots indicates surface roughening while transition from the transmission to the diffraction pattern is the sign of the improvement of surface morphology through the coalescence of neighboring islands.

Polycrystalline films and textured films with no in-plane orientation produce a set of concentric circles, as shown in **Figure 2d**. If some in-plane orientation is present, as in the case of a biaxially textured film, circles break into arcs. In addition, the pattern can consist of a superposition of streaks and spots, as shown for the MgO film in **Figure 3b**. Here, diffraction streaks arise from the epitaxial MgO film and circles are from the randomly oriented MgO inclusions, as was determined from the cross-sectional TEM image shown in **Figure 3c**.

RHEED is also routinely used for the growth rate calibration. If the film grows in a layer-by-layer (Frank-van-der-Merwe) mode, intensity of the diffracted beam oscillates with the frequency proportional to the growth rate. The mechanism of the RHEED intensity oscillations is illustrated in **Figure 4** [5]. Intensity of the beam diffracted by the extremely flat substrate is maximal prior to the growth. As the growth is initiated, scattering from the small two-dimensional islands nucleating on the surface decreases the diffracted beam intensity. It approaches minimum at a half-monolayer coverage that is the roughest stage of the growth. As the first monolayer is complete, the surface flattens again by the coalescence of the islands and diffracted beam intensity recovers. However, since the second monolayer always nucleates before the first is complete, the growth front roughens.

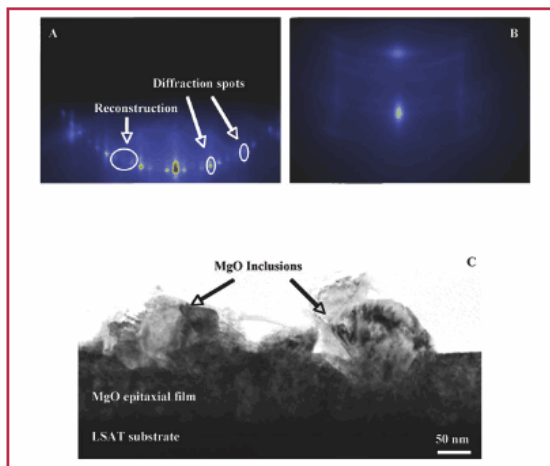


Figure 3. a) RHEED pattern collected from the (100) TiO_2 showing a three-fold reconstruction, b) RHEED pattern collected from the epitaxial MgO film containing randomly-oriented inclusions, c) Cross-sectional TEM image of the same MgO film.

Thus, RHEED oscillations slowly decrease in intensity during the growth, and eventually disappear. Thus, while oscillation frequency is the direct measure of the growth rate, the decay rate provides rich information on the surface mobility of arriving atoms and can be used to study how growth temperature, over-pressure, and / or surfactants influence film growth [6].

Although it is assumed that electrons interact elastically with the crystal lattice, some of them undergo inelastic scattering and loose energy. By adding grids, phosphorus screen can be modified into an electron energy loss detector, allowing combined RHEED-electron energy loss spectroscopy (EELS) measurements [7]. Thus, surface morphology and chemistry can be simultaneously analyzed. In addition, intensive cathodoluminescence (CL) is excited when the direct band gap semiconductor ($\text{Al}_x\text{Ga}_{1-x}\text{N}$, $\text{Zn}_x\text{Cd}_{1-x}\text{Se}$) and oxide ($\text{Zn}_x\text{Mg}_{1-x}\text{O}$) alloys are deposited. CL spectra can be collected either in the imaging mode, via CCD camera equipped with special filters, or in the spectral mode with the luminescence being resolved through the spectrometer and detected by the photomultiplier tube [8]. CL provides additional information on the alloy composition, uniformity, and film quality.

RHEED was originally used only during the high vacuum deposition processes ($< 10^5$ Torr), such as MBE. Two factors limited its application at higher pressures. First, a high gas pressure ($10^5 - 10^3$ Torr) strongly reduced filament lifetime. At even higher pressures ($\sim 10^2$ Torr), increased scattering of electron beam by the gas molecules produced diffuse pattern. However, this limitation was recently overcome through the development of a high-pressure system. At pressures below 10 mTorr, such a system includes a single differential pump next to the electron gun. Due to the high differential pumping efficiency, the pressure in the electron gun is kept at $\sim 10^5$ Torr level even when a chamber pressure is in the 10^{-3} Torr range. A more advanced system, shown in Figure 2b, is used at higher pressures (10 mTorr -100 mTorr) when scattering of electron beam inside the chamber becomes important. The RHEED screen is shifted closer to the sample and

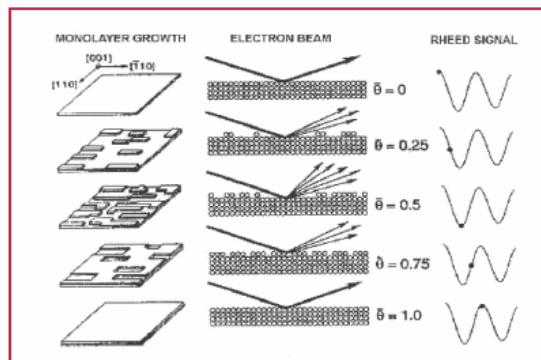


Figure 4. Mechanism of RHEED intensity oscillations during the layer-by-layer growth [5].

a second differential pumping stage is added between the gun and the chamber. A pumped tube protrudes inside the vacuum chamber. The differential pumping aperture at the end of the tube is located close to the substrate. This decreases distance electrons travel through the high-pressure region, allowing efficient RHEED operation even at high pressures [9].

Extended to the high-pressure region, RHEED becomes an invaluable tool for the *in-situ* monitoring during PLD, CVD, and sputtering. High quality differentially-pumped RHEED systems are now available from wide range of companies including *Staub Instruments*, *Pascal Technologies*, and *Twente Solid State Technology*. In addition, a number of excellent books discussing various RHEED aspects in details [10,11] and programs for automatic data acquisition and analysis [12] make this technique extremely user-friendly.

References

1. S. Nishikawa and S. Kikuchi, *Nature* **122**, 726 (1928).
2. M.A. Herman and H. Sitter, *Molecular Beam Epitaxy*, Springer, Berlin (1996).
3. Y. Hida, T. Tamagawa, H. Ueba, C. Tatsuyama, *J. Appl. Phys.* **67**, 7274 (1990).
4. H. J. Osten and J. Klatt, *Appl. Phys. Lett.* **65**, 630 (1994).
5. K. Ploog, *Angewandte Chemie - Int. English Ed.* **27**, 593 (1988).
6. J.M. Van Hove, P.R. Pukite, P.I. Cohen, *J. Vac. Sci. Technol. B* **3**, 563 (1985).
7. W. Braun, L. Däweritz, K. H. Ploog, *Physica E* **2**, 878 (1998).
8. K. Lee, E. D. Schires, T. H. Myers, *Mater. Res. Soc. Symp. Proc.* **892**, 0892-FF04-01.1 (2006).
9. J. Klein, C. Höfener, L. Alff, R. Gross, *Supercond. Sci. Technol.* **12**, 1023 (1999).
10. W. Braun, *Applied RHEED*, Springer, Berlin (1999).
11. A. Ichimiya and P. I. Cohen, *Reflective High Energy Electron Diffraction*, Cambridge University Press, Cambridge (2004).
12. For example, kSa 400 by *K-Space Associates, Inc.*, *SAFIRE* by *CreaTec Fischer & Co.*, and *EZ-RHEED* by *MBE Control Solutions*.